

Polymorphonuclear Neutrophil in Brain Parenchyma After Experimental Intracerebral Hemorrhage

Xiurong Zhao · Guanghua Sun · Han Zhang ·
Shun-Ming Ting · Shen Song · Nicole Gonzales ·
Jaroslaw Aronowski

Received: 20 February 2014 / Revised: 14 March 2014 / Accepted: 17 March 2014 / Published online: 3 April 2014
© Springer Science+Business Media New York 2014

Abstract Polymorphonuclear neutrophils (PMNs) infiltration into brain parenchyma after cerebrovascular accidents is viewed as a key component of secondary brain injury. Interestingly, a recent study of ischemic stroke suggests that after ischemic stroke, PMNs do not enter brain parenchyma and as such may cause no harm to the brain. Thus, the present study was designed to determine PMNs' behavior after intracerebral hemorrhage (ICH). Using the autologous blood injection model of ICH in rats and immunohistochemistry for PMNs and vascular components, we evaluated the temporal and spatial PMNs distribution in the ICH-affected brain. We found that, similar to ischemia, there is a robust increase in presence of PMNs in the ICH-injured tissue that lasts for at least 1 to 2 weeks. However, in contrast to what was suggested for ischemia, besides PMNs that stay in association with the vasculature, after ICH, we found abundance of intraparenchymal PMNs (with no obvious association with vessels) in the ICH core and hematoma border, especially between 1 and 7 days after the ictus. Interestingly, the increased presence of intraparenchymal PMNs after ICH coincided with the massive loss of microvascular integrity, suggesting vascular disruption as a potential cause of PMNs presence in the brain parenchyma. Our study indicates that in contrast to ischemic stroke, after ICH, PMNs target not only vascular compartment but also brain parenchyma in the affected brain. As such, it is possible that the pathogenic role and therapeutic implications of targeting PMNs after ICH could be different from these after ischemic stroke. Our work suggests the needs for more studies addressing the role of PMNs in ICH.

Keywords Intracerebral hemorrhage · Polymorphonuclear neutrophils · Extravasation · Parenchyma

Introduction

Intracerebral hemorrhage (ICH) is a devastating cerebrovascular disease with high mortality and poor prognosis, for which no effective therapies are available [1–3]. The rapid accumulation of blood within the brain parenchyma leads to increased intracranial pressure and brain tissue damage. Local microglia sense the damage and respond with the release of various cytokines and chemokines [4–7], which coordinate the recruitment of blood inflammatory leukocytes. Among these cells, polymorphonuclear neutrophils (PMNs) are considered to be the first to arrive to the hematoma site. Here, they were proposed to cause microvascular plugging and, in an instance of transmigration, lead to direct intraparenchymal brain tissue damage [8–11]. It is considered that shortly after entering the brain parenchyma, PMNs release/discharge an arsenal of highly cytotoxic molecules (e.g., proteases, immune regulation peptides, and reactive oxygen species) that are normally used by PMNs in host-defense activities [12–15]. Although in stroke- and ICH-mediated brain injury [16–19], most of the preclinical studies agree with the overall deleterious role of PMNs; several clinical stroke studies testing therapeutic approaches for stroke based on restricting PMNs' brain entry have been unsuccessful to date due to inefficacy or side-effects such as direct toxicity, leukopenia, and immunosuppression [20–22]. These clinical negative/neutral outcomes intensified the debate over the role of PMNs in stroke pathogenesis [23–27].

Recently, an intriguing study examined (using elegant immunostaining and cell-sorting approaches) the temporal and spatial distribution of PMNs in the human brain tissue after ischemic stroke and in a mouse brain after experimental focal

X. Zhao · G. Sun · H. Zhang · S.-M. Ting · S. Song · N. Gonzales ·
J. Aronowski (✉)
Department of Neurology, Stroke Program, University of
Texas-HSC, Medical School, 6431 Fannin, Suite 7.210, Houston,
TX 77030, USA
e-mail: j.aronowski@uth.tmc.edu

ischemia [28]. It was suggested that although numerous PMNs enter the ischemia-injured brain, the vast majority of them remain closely associated with the vasculature (intraluminal or perivascular). Only a negligible number of PMNs were found in the intraparenchymal tissue (outside of the glia limitans) [28], location where PMNs could inflict most of the damage to the cells of a neurovascular unit. These intriguing findings in ischemic brain inspire us to explore in more details the behavior of PMNs after ICH, a cerebrovascular condition that is pathologically different and often more damaging than ischemic stroke.

Although a few earlier animal studies confirmed presence of PMNs in ICH-affected brain [9, 18, 29–32], our present study focuses on the temporal component of PMNs' brain recruitment and vessel wall integrity. And we evaluate spatial relationship between PMNs and ICH-affected microvessels, over critical 3 weeks after the insult. We are demonstrating that the PMNs number increases over the first 3 days after ICH in the ICH-affected brain and that PMNs infiltrate both the perivascular space and, in contrast to ischemic stroke [28], the brain's intraparenchymal tissue. The intraparenchymal presence of PMNs antecede or coincides with the loss of microvessels, suggesting that the extravascular PMNs may not only be the consequence of the receptor-mediated transmigration but also be a result of loss of the physical barrier—vessel wall.

Materials and Methods

Animal Preparation and Intracerebral Hemorrhage (ICH) Model in Rat

All the animal studies followed the guidelines outlined in *Guide for the Care and Use of Laboratory Animals* from the National Institutes of Health and were approved by the University of Texas-Houston Health Science Center Animal Welfare Committee.

The ICH in 60 male Sprague–Dawley rats (Harlan) (250–350 g) was induced by intra-striatal infusion of autologous blood, as we described previously [33–36]. This protocol produces injury that results in pronounced neurological deficit. Briefly, under 0.35 g/kg chloral hydrate anesthesia, the rats were immobilized onto a stereotaxic frame. One-millimeter-diameter burr hole was drilled in the skull, and a 22-G stainless steel blunt cannula was inserted at 0.7 mm anterior and 3 mm lateral from the bregma and 3 mm deep from skull for the blood (collected from femoral artery, right before blood infusion) infusion (35 μ l over 5 min) into the left corpus striatum. This approach leads to the infiltration of blood into adjacent neuropil which at closer look forms a heterogeneous mixture (mosaic) of blood and brain tissue (Fig. 2b), not just a

large bulk of blood. The animals were analyzed at 1, 3, 6, 24, 48, 72 h, 7, 14, and 21 days after surgery.

Animal Perfusion and Immunofluorescence

The animals were anesthetized with isoflurane and intracardially perfused with ice-cold PBS. The harvested brains were immediately frozen in 2-methylbutane on dry ice and then stored at -80°C prior to cryosectioning into coronal 10- μ m-thick sections. The sections were treated with 95 % methanol containing 5 % acetic acid at -20°C for 10 min, as we described [36], and then permeabilized in 0.3 % NP-40 and blocked in 1 % normal goat serum in PBS. The rabbit anti-human myeloperoxidase (MPO) (DAKO, A0398; 1:1,000), mouse anti-rat RP-1 (BD Pharmingen, 550000; 1:1,000), rabbit anti-laminin (Novus Biological, NB300-144; 1:2,000), rabbit anti-rat red blood cells (RBC, Fitzgerald, 60R-RR009FT; 1:2,000), mouse anti-rat CD31 (BD Pharmingen, 550300; 1:500), or mouse anti-RECA-1 (Abcam, ab9774; 1:500) was applied to the brain sections and incubated at 4°C overnight. For double immunofluorescence of laminin/RP-1, laminin/CD31, or laminin/RECA-1, both primary antibodies were simultaneously applied onto the sections and incubated at 4°C overnight. The signals were visualized using goat anti-mouse or anti-rabbit IgG conjugated to either Alexa-Fluor-488 or Alexa-Fluor-546 (Molecular Probes 1:200). The tissue sections were covered with the anti-fade mount medium containing 4',6-diamidino-2-phenylindole (DAPI) (Invitrogen).

Image Capture and Cell/Vessels Counting

A Zeiss Axioskop-2 microscope equipped with CCD camera and operated with MetaMorph 6.2 software was used for image acquisition. The fluorescence-labeled cells are visualized using Ex/Em of 490/520 nm for Alexa 488, Ex/Em of 550/575 nm for Alexa 546, and Ex/Em of 365/480 nm for DAPI. To avoid sampling bias during cell/vessel counting, we took advantage of the montage element that allows stitching the images (acquired through 10 \times objective), an approach allowing for counting immunopositive PMNs (MPO or RP-1) or vessels (laminin) across the ICH-affected hemisphere. Three 10- μ m-thick sections through the ICH-affected tissue (one at the needle insertion site—0.7 mm anterior to the bregma, and one at 0.25 mm anterior and one at 0.25 mm posterior from the needle insertion site) were generated for the data analyses. Five randomly selected rats were analyzed per each time point. The number of PMNs in an ICH-affected hemisphere was counted automatically with the assistance of the MetaMorph program. The total number of PMNs in three sections from each brain was calculated and expressed as mean \pm SEM. The number of blood vessels in naïve or ICH-affected rat brains was achieved by manual counting vessels

projected on the computer screen. The vessel counting reflects the overall number of individual immunolabeled vessels within the area of 0.6 mm [2] representing a hematoma-affected brain (core and borders).

Statistical Analysis

The results were analyzed using the GraphPad and InStat programs and are expressed as mean±SEM. One-way analysis of variance (ANOVA) with a Newman–Keuls posttest was used for multiple comparisons. The statistical significance was considered at $P \leq 0.05$.

Results

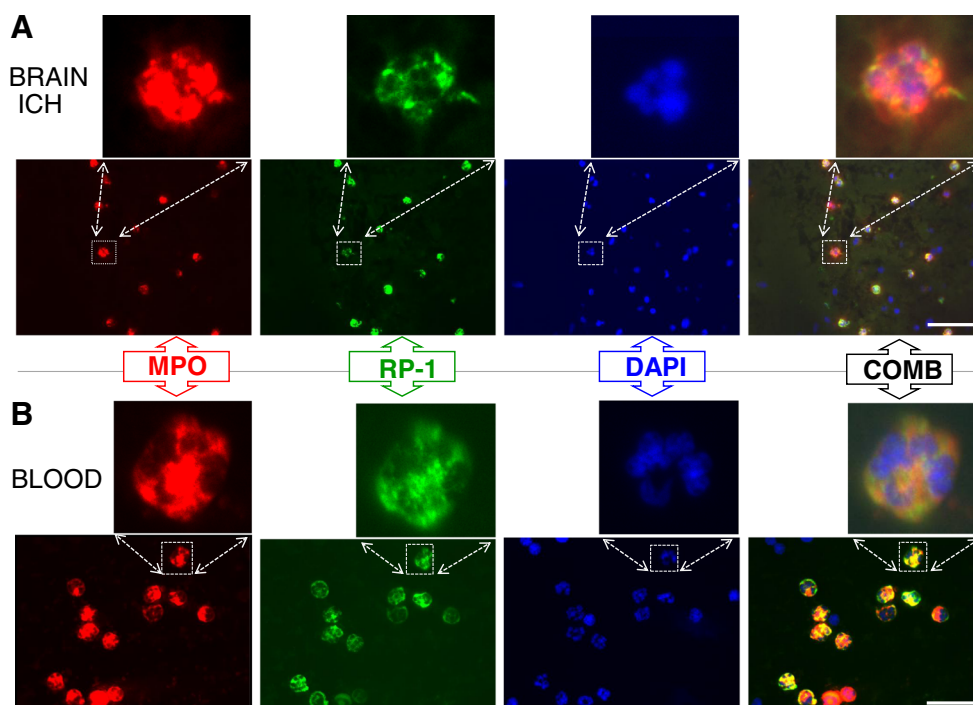
PMN Infiltration into Brain After ICH

Myeloperoxidase (MPO) is an abundant constituent of PMNs' primary granules that is frequently employed as a sensitive and considerably selective marker for PMNs from their promyelocyte to the mature stage [37]. In addition to MPO, RP-1 emerged recently as a reliable antigen for selective recognition of rat segmented and band PMNs [38, 39]. Thus, in our initial studies, to confirm the reliability of the PMNs staining with antibodies recognizing these two antigens, we demonstrated that in brain tissue after ICH, both anti-MPO and RP-1 antibodies label the same population of cells (double immunofluorescence experiment; Fig. 1a). We further showed that these MPO and RP-1 immunopositive cells also

demonstrate multi-lobed nuclear morphology (visualized using labeling of nuclear DNA with DAPI) similar to that of MPO- and RP-1-positive neutrophils from peripheral blood (Fig. 1a, b; DAPI). Although MPO was earlier shown to localize to lysosomes of some macrophages [40, 41], the staining intensity for MPO in the CD68-positive or OX42-positive cells (markers for microglia/macrophages) in the ICH-affected brain was dramatically weaker (basically undetectable), as compared to the signal in RP-1-positive PMNs (data not included), reassuring that under condition of our experiments both MPO and RP-1 antigens are reliable markers of PMNs in our morphological studies.

Next, using RP-1 staining, we characterized the temporal and spatial PMNs' profile in the ICH-affected brain. In agreement with the existing notion, we found that there are no PMNs in the naïve-perfused rat brain (Fig. 2a). Also, we established that intracerebral injection of saline (instead of blood) results in a negligible neutrophil response in the area that is solely adjacent to the needle track (used to inject blood), which is likely the result of mechanical tissue disruption caused by the stereotaxic surgery (not shown). At 1 and 3 h after ICH, we consistently detected an occasional (3–4 cells per cross section through ICH brain) presence of PMNs that were strictly confined to the hematoma mass. Based on their homogenous distribution and location within the hematoma mass, we believe that these cells most likely represent PMNs that were injected with the blood to produce ICH. It was not until 6 h after ICH when we detected a clear increase in number of PMNs in the hematoma-affected hemisphere (Fig. 2a), both within the ICH core (defined by not only

Fig. 1 MPO (red) and RP-1 (green) label the same cell population **a** in the brain at 24 h after ICH and **b** in purified blood PMN. The nuclei are stained with DAPI (blue). *Comb* is an overlay of MPO/RP-1/DAPI stain. Note that the nuclei are multilobal, feature typical for PMNs. The PMNs attached to glass slide appear larger than their brain counterpart. Scale bar 30 μ m



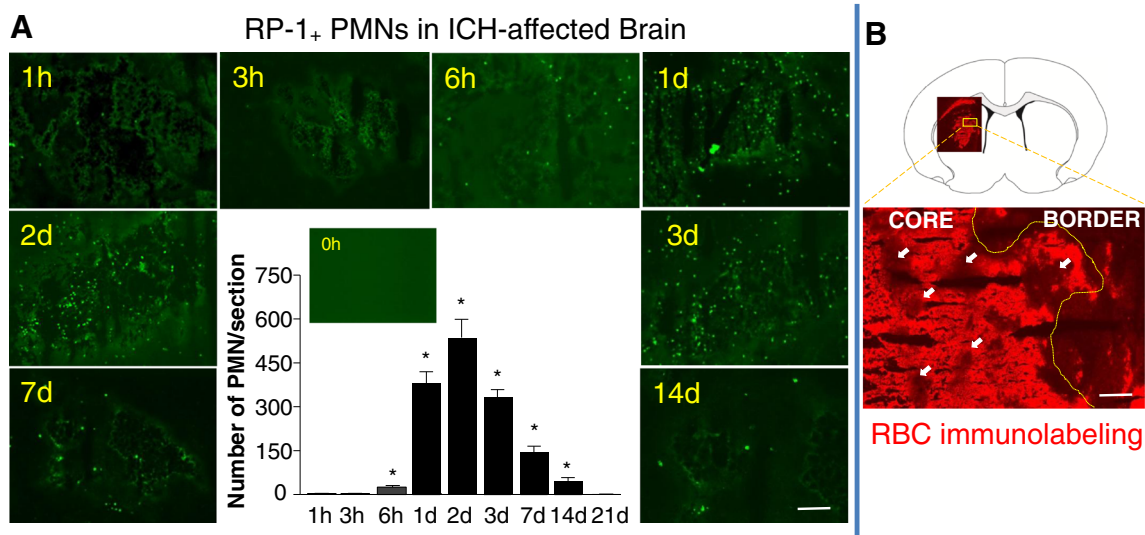


Fig. 2 a Time course demonstrating number of PMNs present in the ICH-affected rat brain at 0 to 21 days. Scale bar 50 μ m. The total number of RP-1 immunopositive PMNs (green) in each brain was counted in three coronal sections generated from ICH-affected brain representing the needle insertion level (blood injection site), and 0.25 mm anterior/posterior to this site. The data are displayed as mean \pm SEM ($n=5$ rats/time point). * $P \leq 0.05$, compared with the number of PMNs at 1 h. **b** Immunostaining of RBC (red) was employed to identify hematoma and its borders. Scale bar 50 μ m. Note presence of small patches (white arrows) of tissue devoid of RBC within the hematoma core

immunostaining with anti-RBC antibody as a region composed primarily of blood, but also consisting of patches of brain tissue between blood; Fig. 2b) and the hematoma border (neuropil that is directly adjacent to the hematoma mass; Fig. 2b). In the course of consecutive 3 days, the total number of PMNs in ICH-affected tissue robustly increased, followed by the gradual decline over 2 weeks (Fig. 2a). There were no PMNs present in the brain at 3 weeks after ICH. No MPO- or RP-1-positive cells were detected in the contralateral hemisphere at any of the time points.

Vascular Disruption in Brain After ICH

Since one of the primary goals of this study was to establish the relationship between brain's PMNs and vascular status quo, we next investigated the impact of ICH on microvascular integrity. To visualize the changes in microvascular structure and distribution in the hematoma-compromised brain, we used immunohistochemistry and a pan-laminin antibody, which react with both laminin-1 ($\alpha 1$, $\beta 1$, and $\gamma 1$) and laminin-2 ($\alpha 2$, $\beta 1$, and $\gamma 1$). This antibody labels all the brain vessels (including capillaries) [42]. Since laminin could theoretically be degraded by proteases generated in response to ICH-induced injury (thereby losing capacity to serve as tracer for the vessels), in selected experiments, to exclude such possibility, we showed that laminin marks the same set of vessels as RECA-1 and anti-CD31 antibodies (tracers commonly used for labeling vessels [43–45]) including after ICH (Fig. 3a, b).

In the naïve rat brain or in the contralateral to ICH hemisphere, blood vessels are evenly distributed throughout the

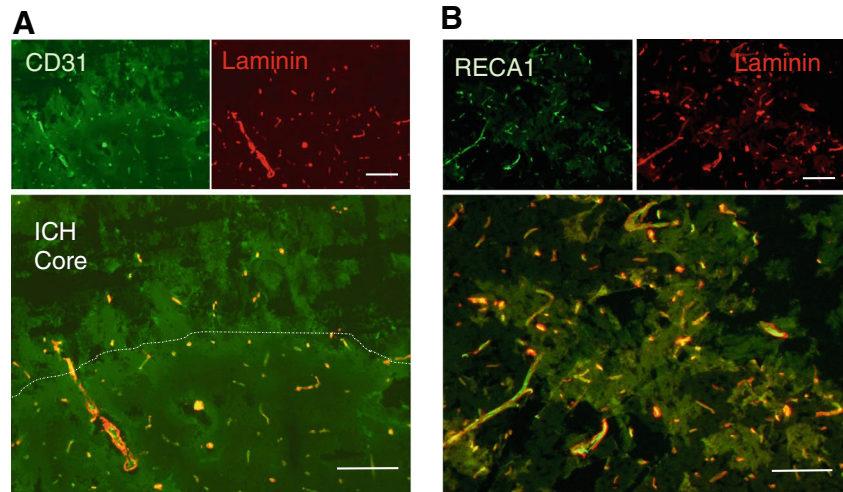
striatal tissue (Fig. 4a). This homogenous vascular pattern was significantly disrupted by the ICH. As early as 1–6 h after ICH, vessels within the hematoma core or hematoma periphery showed some swelling and displayed morphology suggestive of fragmentation (Fig. 4a). This coincided with the local loss of BBB integrity as assessed by increased albumin permeability (not shown). The disruption of the vascular bed gradually progressed over the consecutive 3 days after ICH (Fig. 4a, b). By day 3, only scarce vessels remained in the hematoma core and its immediately adjacent border. Finally, by day 7, new vessels started to appear, initially at the hematoma borders and then gradually extending toward the areas occupied by hematoma core over the next 2–3 weeks after ICH.

posterior to this site. The data are displayed as mean \pm SEM ($n=5$ rats/time point). * $P \leq 0.05$, compared with the number of PMNs at 1 h. **b** Immunostaining of RBC (red) was employed to identify hematoma and its borders. Scale bar 50 μ m. Note presence of small patches (white arrows) of tissue devoid of RBC within the hematoma core

Vasculature Disruption and PMNs Infiltration

To establish the relationship between blood brain vasculature and PMNs in the ICH-affected brain, we used RP-1/laminin double immunofluorescence. In the carefully perfused rat brains after ICH, we consistently found that PMNs accumulate on the luminal surfaces and in the perivascular space of blood vessels (Fig. 5a, b), as well as in the brain parenchyma (locations showing no association with the vessels; Fig. 5c, e). At the earlier time points, e.g., at 1–3 days after ICH, a preponderance of PMNs were found to be scattered throughout the hemorrhagic areas (within the hematoma core as well as at the adjacent hematoma border) and have no clear association with the surrounding vessels—laminin-outlined structures. Besides, we observed numerous PMNs that demonstrated an obvious association with the brain vessels (Fig. 5a, e).

Fig. 3 CD31 (a) and RECA-1 (b) (green)-labeled endothelium and laminin (red)-labeled basal lamina (to outline cerebral vessels) shows complete overlap in the ICH-affected brain hemisphere, as demonstrated here at 24 h after the ICH onset. Scale bar 50 μ m



By day 7, intraparenchymal PMNs were still present, but their manifestation was less prevalent and primarily confined to larger vessels at the hematoma borders (Fig. 5e).

Discussion

PMNs in the ICH-affected brain have been studied for several decades and are often viewed as one of the central features of inflammation-mediated brain damage [8, 9, 13, 15, 29, 32, 46, 47]. It is assumed that after brain injury, PMNs that are attracted to the damaged site could not only mechanically plug affected brain microvessels (contributing to so called no-reflow phenomenon) but also cause direct biochemical

injury following transmigration to the brain parenchyma [8, 13, 15]. PMNs that entered the brain parenchyma can generate large quantities of free radicals (primarily via NADPH-oxidase and MPO) and release various proteases (e.g., cathepsin G, elastase, proteinase 3, or MMP-9), which may degrade extracellular matrix and produce damage to vessels (including loss of BBB integrity), neurons, and other cells within the neurovascular unit [15, 48]. Unexpectedly, recent histological studies of the brain after ischemic stroke by Enzman et al [28] posed fundamental questions regarding the pervasiveness of PMNs' extravasation and their damaging effect toward the neurovascular unit. Using brain tissues derived from mouse subjected to focal ischemia or brain tissue from humans after ischemic stroke and the carefully executed histological

Fig. 4 Time course of vascular loss in the ICH-affected brain at 1 h–21 days after ICH. **a** Representative images of laminin-positive vessels in naïve and ICH-affected striatum. Scale bar 50 μ m. **b** Bar graph showing vascular loss in the ICH-affected striatum. The numbers of vessels was counted in three coronal sections (as in Fig. 2) for each ICH-affected brain and are displayed as percentage changes over the naïve animals. The data are expressed as mean \pm SEM ($n=5$ rats). * $P<0.05$, compared with naïve animal

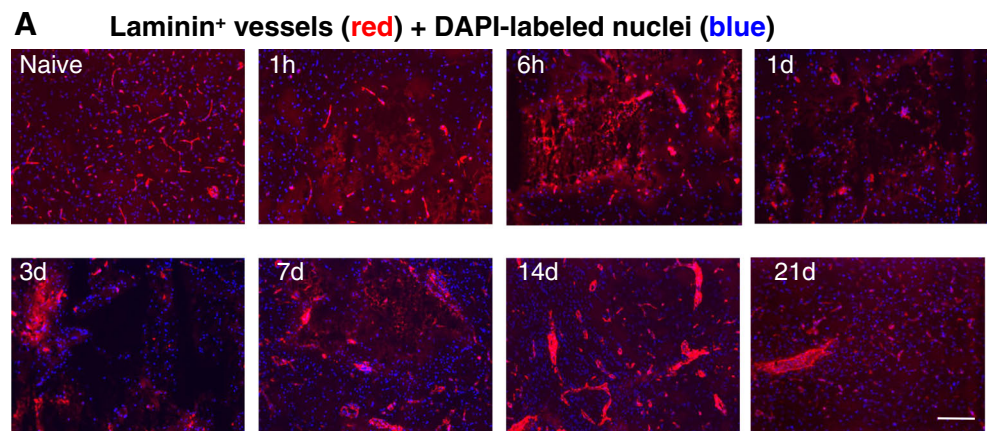
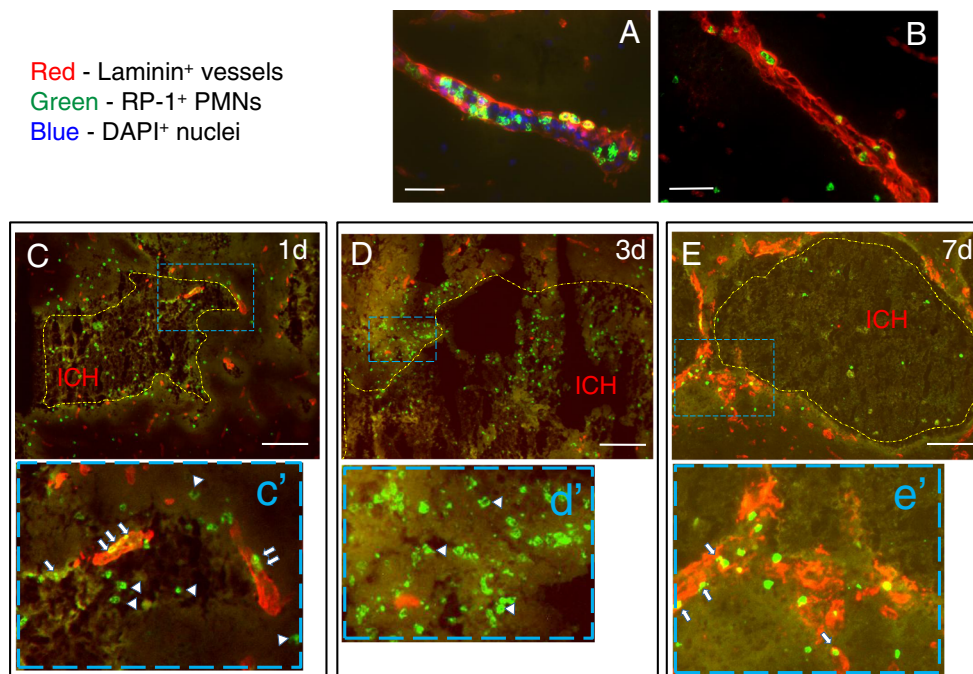


Fig. 5 a–e Representative images illustrating the spatial relationship between RP-1 labeled PMNs (green) and laminin-labeled vessels (red) in the ICH-affected rat brain at day 1 (a–c), 3 (d), and 7 (e) after ICH. Dashed yellow lines (c–e) outline the location of hematoma core (ICH). Blue dashed rectangles outlines the areas that are enlarged in the images (c–e) showed immediately below. White arrows point at PMNs in the vessel. White arrowheads point at PMNs that have no association with the vasculature. Scale bar 50 μ m



approaches, these authors proposed that although PMNs are localized intraluminally and in the perivascular space of cerebral vessels, they were unfrequently present (or not present at all) in the infarcted brain parenchyma. Since PMNs, which entered the brain parenchyma, are viewed as a source on tissue injury, this finding raises many questions and suggests a need for more careful analysis of PMNs in other cerebrovascular diseases—that includes ICH.

Thus, in the present study, using specific makers for PMNs and blood vessels, we analyzed the temporal and spatial distribution of PMNs in brain tissue after intraparenchymal injection of autologous blood in rat, a common and clinically relevant animal model of human ICH [3, 35]. Our data strongly suggest that in the ICH-affected brain, the landscape of PMNs behavior could be strikingly different regarding intraparenchymal presence of PMNs. Following either the ischemic stroke [28] or ICH (present study), PMNs can be readily seen within the vascular lumen and in the perivascular space (demarcated by glia limitans) of cerebral vessels. We found an initial increase in the number of PMNs in the ICH-affected brain as early as 6 h after the onset of injury, delay which is similar to that reported for ischemic stroke [28]. PMNs infiltration peaked between 1 and 3 days, which is again similar to what is reported for ischemic stroke, 8–24 h [28]. Intriguingly, the most notable feature of the ICH-affected brain histology was that unlike what is reported for ischemic stroke [28], we found the abundance of PMNs in the intraparenchymal tissue. This morphological feature was most notable between day 1 and 3 after ICH and coincided with the clear loss of vasculature in the hematoma-affected tissue. A cause of the observed vascular loss remains speculative, as

much as the role it plays in PMNs' extravasation. It was suggested, that following ischemia, the intravascular accumulation of PMNs in the affected brain vessels has no direct impact on vascular integrity, as evidenced by the intact BBB integrity [28]. Thus, it is likely that the vascular accumulation of PMNs after ICH may similarly have no immediate impact on the vascular damage. Interestingly, Enzman et al. [28] also noted that although PMNs are seldom present in the parenchyma of ischemic brain, their intraparenchymal presence was noted in case the ischemic tissue showed evidence of hemorrhagic transformation [28]. This intriguing observation, together with the results of our present study, raises a possibility that the displaced blood components pushed to extravascular space may be causally related to PMNs extravasation. During hematoma formation, blood passes through the perivascular space to the brain parenchyma where it can trigger inflammation, chemokine production, and PMN recruitment to the ICH-affected brain. Consequently, blood- and proinflammatory factors-mediated oxidative stress and proteolytic stress may lead to the disruption of continuity of vessels and PMNs leakage to the intraparenchymal space. This scenario appears to be in line with our present findings that the presence of PMNs in intraparenchymal space corresponded to the territory demonstrating loss of the vasculature in the ICH-affected brain, and especially core.

Ultimately, our studies suggest that ICH triggers a robust PMNs recruitment to the injured brain and that many of these recruited PMNs enter the brain parenchyma, a location where PMNs may impose direct injury to all cells comprising the neurovascular unit. This difference in pathogenesis of ICH strongly suggests that the therapeutic approaches aiming at

limiting PMNs recruitment to the injured brain could be more beneficial when applied to ICH as compared to ischemic stroke.

Acknowledgments This work was partially supported by the National Institutes of Health, NINDS grants NS060768 and NS064109.

Compliance with Ethics Requirements All institutional and national guidelines for the care and use of laboratory animals were followed.

Conflict of Interest All authors declare no conflict of interest.

References

- Qureshi AI, Mendelow AD, Hanley DF. Intracerebral haemorrhage. *Lancet*. 2009;373:1632–44.
- Aronowski J, Zhao X. Molecular pathophysiology of cerebral hemorrhage: secondary brain injury. *Stroke*. 2011;42:1781–6.
- Keep RF, Hua Y, Xi G. Intracerebral haemorrhage: mechanisms of injury and therapeutic targets. *Lancet Neurol*. 2012;11:720–31.
- Ravichandran KS. Find-me and eat-me signals in apoptotic cell clearance: progress and conundrums. *J Exp Med*. 2010;207:1807–17.
- Elliott MR, Ravichandran KS. Clearance of apoptotic cells: implications in health and disease. *J Cell Biol*. 2010;189:1059–70.
- Chekeni FB, Ravichandran KS. The role of nucleotides in apoptotic cell clearance: implications for disease pathogenesis. *J Mol Med (Berlin)*. 2011;89:13–22.
- Aronowski J, Hall CE. New horizons for primary intracerebral hemorrhage treatment: experience from preclinical studies. *Neurol Res*. 2005;27:268–79.
- del Zoppo GJ, Schmid-Schonbein GW, Mori E, Copeland BR, Chang CM. Polymorphonuclear leukocytes occlude capillaries following middle cerebral artery occlusion and reperfusion in baboons. *Stroke*. 1991;22:1276–83.
- Gong C, Hoff JT, Keep RF. Acute inflammatory reaction following experimental intracerebral hemorrhage in rat. *Brain Res*. 2000;871:57–65.
- Weston RM, Jones NM, Jarrott B, Callaway JK. Inflammatory cell infiltration after endothelin-1-induced cerebral ischemia: histochemical and myeloperoxidase correlation with temporal changes in brain injury. *J Cereb Blood Flow Metab*. 2007;27:100–14.
- Jin R, Yang G, Li G. Inflammatory mechanisms in ischemic stroke: role of inflammatory cells. *J Leukoc Biol*. 2010;87:779–89.
- Soehnlein O. An elegant defense: how neutrophils shape the immune response. *Trends Immunol*. 2009;30:511–2.
- Garcia JH, Liu KF, Yoshida Y, Lian J, Chen S, del Zoppo GJ. Influx of leukocytes and platelets in an evolving brain infarct (Wistar rat). *Am J Pathol*. 1994;144:188–99.
- Matsuo Y, Kihara T, Ikeda M, Ninomiya M, Onodera H, Kogure K. Role of neutrophils in radical production during ischemia and reperfusion of the rat brain: effect of neutrophil depletion on extracellular ascorbyl radical formation. *J Cereb Blood Flow Metab*. 1995;15:941–7.
- Kalimo H, del Zoppo GJ, Paetau A, Lindsberg PJ. Polymorphonuclear neutrophil infiltration into ischemic infarctions: myth or truth? *Acta Neuropathol*. 2013;125:313–6.
- Dawson DA, Ruetzler CA, Carlos TM, Kochanek PM, Hallenbeck JM. Polymorphonuclear leukocytes and microcirculatory perfusion in acute stroke in the SHR. *Keio J Med*. 1996;45:248–52. discussion 252–243.
- Hallenbeck JM, Dutka AJ, Tanishima T, Kochanek PM, Kumaroo KK, Thompson CB, et al. Polymorphonuclear leukocyte accumulation in brain regions with low blood flow during the early postischemic period. *Stroke*. 1986;17:246–53.
- Sansing LH, Harris TH, Kasner SE, Hunter CA, Kariko K. Neutrophil depletion diminishes monocyte infiltration and improves functional outcome after experimental intracerebral hemorrhage. *Acta Neurochir Suppl*. 2011;111:173–8.
- Loftspring MC, Johnson HL, Johnson AJ, Clark JF. Depletion of gr-1-positive cells is associated with reduced neutrophil inflammation and astrocyte reactivity after experimental intracerebral hemorrhage. *Transl Stroke Res*. 2012;3:147–54.
- Investigators EAST. Use of anti-icam-1 therapy in ischemic strokes: results of the enlimomab acute stroke trial. *Neurology*. 2001;57:1428–34.
- Becker KJ. Anti-leukocyte antibodies: Leukarrest (hu23f2g) and enlimomab (r6.5) in acute stroke. *Curr Med Res Opin*. 2002;18(2):s18–22.
- Krams M, Lees KR, Hacke W, Grieve AP, Orgogozo JM, Ford GA. Acute stroke therapy by inhibition of neutrophils (astin): an adaptive dose-response study of UK-279,276 in acute ischemic stroke. *Stroke*. 2003;34:2543–8.
- Beray-Berthat V, Palmier B, Plotkine M, Margaill I. Neutrophils do not contribute to infarction, oxidative stress, and no synthase activity in severe brain ischemia. *Exp Neurol*. 2003;182:446–54.
- Emerich DF, Dean 3rd RL, Bartus RT. The role of leukocytes following cerebral ischemia: pathogenic variable or bystander reaction to emerging infarct? *Exp Neurol*. 2002;173:168–81.
- Fassbender K, Ragooschke A, Kuhl S, Szabo K, Fatar M, Back W, et al. Inflammatory leukocyte infiltration in focal cerebral ischemia: unrelated to infarct size. *Cerebrovasc Dis*. 2002;13:198–203.
- Hayward NJ, Elliott PJ, Sawyer SD, Bronson RT, Bartus RT. Lack of evidence for neutrophil participation during infarct formation following focal cerebral ischemia in the rat. *Exp Neurol*. 1996;139:188–202.
- Takeshima R, Kirsch JR, Koehler RC, Gomoll AW, Traystman RJ. Monoclonal leukocyte antibody does not decrease the injury of transient focal cerebral ischemia in cats. *Stroke*. 1992;23:247–52.
- Enzmann G, Mysiorek C, Gorina R, Cheng YJ, Ghavampour S, Hannocks MJ, et al. The neurovascular unit as a selective barrier to polymorphonuclear granulocyte (PMN) infiltration into the brain after ischemic injury. *Acta Neuropathol*. 2013;125:395–412.
- Moxon-Emre I, Schlichter LC. Neutrophil depletion reduces blood-brain barrier breakdown, axon injury, and inflammation after intracerebral hemorrhage. *J Neuropathol Exp Neurol*. 2011;70:218–35.
- Patel S, de la Fuente J, Atra A, Senevirathne S, Cale CM. Where have all the neutrophils gone? *Arch Dis Child Educ Pract Ed*. 2009;94:74–7.
- Yang S, Nakamura T, Hua Y, Keep RF, Younger JG, He Y, et al. The role of complement C3 in intracerebral hemorrhage-induced brain injury. *J Cereb Blood Flow Metab*. 2006;26:1490–5.
- Xue M, Del Bigio MR. Intracerebral injection of autologous whole blood in rats: time course of inflammation and cell death. *Neurosci Lett*. 2000;283:230–2.
- Zhao X, Sun G, Zhang J, Strong R, Song W, Gonzales N, et al. Hematoma resolution as a target for intracerebral hemorrhage treatment: role for peroxisome proliferator-activated receptor gamma in microglia/macrophages. *Ann Neurol*. 2007;61:352–62.
- Hickenbottom SL, Grotta JC, Strong R, Denner LA, Aronowski J. Nuclear factor-kappaB and cell death after experimental intracerebral hemorrhage in rats. *Stroke*. 1999;30:2472–7. discussion 2477–2478.
- Felberg RA, Grotta JC, Shirzadi AL, Strong R, Narayana P, Hill-Felberg SJ, et al. Cell death in experimental intracerebral hemorrhage: the “black hole” model of hemorrhagic damage. *Ann Neurol*. 2002;51:517–24.
- Zhao X, Zhang Y, Strong R, Grotta JC, Aronowski J. 15d-prostaglandin j2 activates peroxisome proliferator-activated receptor-gamma, promotes expression of catalase, and reduces inflammation, behavioral

- dysfunction, and neuronal loss after intracerebral hemorrhage in rats. *J Cereb Blood Flow Metab.* 2006;26:811–20.
37. Pinkus GS, Pinkus JL. Myeloperoxidase: a specific marker for myeloid cells in paraffin sections. *Mod Pathol.* 1991;4:733–41.
 38. Gotoh S, Itoh M, Fujii Y, Arai S, Sendo F. Enhancement of the expression of a rat neutrophil-specific cell surface antigen by activation with phorbol myristate acetate and concanavalin a. *J Immunol.* 1986;137:643–50.
 39. Skrajnar S, Anzur Lasnik M, Bedina ZA. A flow cytometric method for determination of the blood neutrophil fraction in rats. *J Am Assoc Lab Anim Sci.* 2009;48:152–6.
 40. Arkema JM, Schadee-Eestermans IL, Beelen RH, Hoefsmit EC. A combined method for both endogenous myeloperoxidase and acid phosphatase cytochemistry as well as immunoperoxidase surface labelling discriminating human peripheral blood-derived dendritic cells and monocytes. *Histochemistry.* 1991;95:573–8.
 41. de Mendez I, Young Jr KR, Bignon J, Lambre CR. Biochemical characteristics of alveolar macrophage-specific peroxidase activities in the rat. *Arch Biochem Biophys.* 1991;289:319–23.
 42. Lifshitz V, Benromano T, Weiss R, Blanga-Kanfi S, Frenkel D. Insulin-degrading enzyme deficiency accelerates cerebrovascular amyloidosis in an animal model. *Brain Behav Immun.* 2012
 43. Tu YF, Tsai YS, Wang LW, Wu HC, Huang CC, Ho CJ. Overweight worsens apoptosis, neuroinflammation and blood–brain barrier damage after hypoxic ischemia in neonatal brain through JNK hyperactivation. *J Neuroinflammation.* 2011;8:40.
 44. Wang LW, Tu YF, Huang CC, Ho CJ. JNK signaling is the shared pathway linking neuroinflammation, blood–brain barrier disruption, and oligodendroglial apoptosis in the white matter injury of the immature brain. *J Neuroinflammation.* 2012;9:175.
 45. Williams KC, Zhao RW, Ueno K, Hickey WF. Pecam-1 (CD31) expression in the central nervous system and its role in experimental allergic encephalomyelitis in the rat. *J Neurosci Res.* 1996;45:747–57.
 46. Wang J, Tsirka SE. Tuftsin fragment 1–3 is beneficial when delivered after the induction of intracerebral hemorrhage. *Stroke.* 2005;36:613–8.
 47. Wasserman JK, Schlichter LC. Neuron death and inflammation in a rat model of intracerebral hemorrhage: effects of delayed minocycline treatment. *Brain Res.* 2007;1136:208–18.
 48. Amulic B, Cazalet C, Hayes GL, Metzler KD, Zychlinsky A. Neutrophil function: from mechanisms to disease. *Annu Rev Immunol.* 2012;30:459–89.